ELSEVIER

Catalysis Today 43 (1998) 51–67

CATALYSIS TODAY

A homogeneously dispersed silica dopant for control of the textural and structural evolution of an alumina aerogel

James B. Miller[1], Edmond I. Ko[*]

Department of Chemical Engineering, Carnegie Mellon University, Pittsburgh, PA 15213-3890, USA

Abstract

We have prepared pure alumina and silica-doped alumina (9:1 Al:Si atom ratio) aerogels by supercritical drying of monolithic alcogels formed by slow, sub-stoichiometric (H_2O:Al=2.2) hydrolysis of solutions of alkoxide precursors (aluminum *s*-butoxide and tetraethyl orthosilicate) in *s*-butanol. Both aerogels were X-ray indifferent over a large temperature range, first ordering as the η transition form upon calcination at 1173 K. The silica dopant retarded sintering of the aerogel, thereby enhancing its surface area and delaying crystallization of α-alumina from 1373–1473 K. Silica did not, however, affect the surface-chemical properties of the X-ray amorphous alumina; both aerogels were inert to pyridine adsorption and butene isomerization probes at 523 K. Stabilization of structure and texture without alteration of surface-chemical properties is a result of the high dispersion of the silica dopant throughout the aerogel's bulk. Incorporation of silicon atoms into the growing pre-alumina network facilitates their insertion into vacancies in the transition alumina structure, thereby restricting lattice diffusion as a route for crystallization of the α phase.

Keywords: Alumina aerogels; Penta-coordinated aluminum; Silica-doped alumina

1. Introduction

1.1. Aluminas in high-temperature applications

The large surface areas and porosities of the transition aluminas account for their wide use as catalyst supports. The transition forms are, however, metastable; at temperatures in excess of 1300 K, they begin to crystallize to the thermodynamically stable; α (or corundum) phase [1–4]. This transformation is accompanied by catastrophic surface area and pore volume loss, effectively limiting the usefulness of the alumina in high-temperature catalytic applications. The textural properties of transition aluminas are, therefore, functions of the rates at which structural transformations take place upon heat treatment. The precise order of transformations and temperatures at which they occur depend, in turn, upon the details of the preparation of alumina [1–4]. Understanding the transformation kinetics, and how they may be controlled by preparation, is important for extending the operating range of alumina for applications like catalytic combustion that can require long operating times at temperatures as high as 1500 K [5,6].

To retard sintering processes and delay crystallization, transition aluminas and their precursors have

*Corresponding author. Present address: City University of Hong Kong, Kowloon, Hong Kong.

[1]Present address: Mine Safety Appliances Company, P.O. Box 427, Pittsburgh, PA 15230, USA.

0920-5861/98/$32.00
PII S0920-5861(98)00134-5

been successfully doped with various materials, especially rare earths and alkaline earth metals. Silica, introduced both within the alumina's structure as a co-precipitate or co-gel [7–9], and on its surface by grafting and related techniques [9–11], has also been reported to be an effective dopant; depending on the amount of silica and the details of preparation, crystallization of α can be delayed by as much as $\sim$200 K [7] and surface areas as high as $\sim$100 m^2/g after heat treatment at 1473 K can be preserved [8]. However, silica's propensity to impart undesirable surface-chemical characteristics, most notably surface acidity, has limited its use in combustion-related applications [5]. For all dopants, the mechanisms responsible for the stabilization of low temperature structures and high surface areas remain unclear. For silica, in particular, the differences between surface- and bulk-modified materials are not well understood.

1.2. *Structural and textural evolution of alumina precursors*

The transition sequence (or structural evolution) of alumina precursors prepared by precipitation from aqueous solutions of aluminum salts has been thoroughly studied and is well understood [1,4,12]. Gelatinous aluminum hydroxides precipitated from aqueous solutions initially display no medium- or long-range order, i.e., they are X-ray indifferent. But, during the relatively mild hydrothermal conditions encountered during counterion removal and drying, the precipitates usually transform to well ordered aluminum oxidehydroxides (boehmite, for example) or trihydroxides (bayerite, gibbsite); the form that appears depends, again, upon the details of the preparation [1]. Less common are drying schedules that preserve the disorder of the initial precipitate [1,12].

Upon thermal treatment at moderate temperatures (600–800 K), the ordered aluminum hydroxides dehydrate to form the 'transition aluminas'– η, γ, θ and others [1–4]. The transition aluminas are not equilibrium phases, but rather reproducible, kinetically stabilized forms [1–3]. The transformation from hydroxide to transition form is topotactic: it takes place over very short transport distances, maintaining the hydroxide's cubic-close-pack oxygen sub-lattice [1,3]. The result is that the hydroxide loses significant mass upon dehydration, but without an accompanying change in the external dimensions of the crystallite. The intracrystalline micropores that form are responsible for the high surface areas of the transition aluminas [1,3]. At high heat-treatment temperatures (>1300 K) the transition aluminas crystallize to the thermodynamically stable α, or corundum, phase.

Alumina precursors have also been prepared by hydrolysis of alkoxides ($Al(OR)_3$) in non-aqueous solvents. Variants of this approach that employ high hydrolysis ratios ($\sim$100 mol H_2O/mol Al) deliver the well-ordered oxidehydroxides and trihydroxides either as primary products or after a short, low-temperature aging period [1,3]. Aside from their improved purity, these aluminas are fundamentally the same as those prepared from aqueous salt solutions; they transform according to the same sequences. Having received significantly less attention are alumina precursors prepared from alkoxides at near, or sub-stoichiometric (with respect to the trihydroxide: $Al(OR)_3+3H_2O \rightarrow Al(OH)_3+3ROH$) water ratios [12]. This approach, combined with the supercritical solvent removal, has been employed to deliver X-ray indifferent aerogels [13–15]. The X-ray amorphous form can exist to temperatures as high as 1200 K, where it enters the transition sequence, typically as η-alumina. While the water ratio (mols H_2O/mol aluminum alkoxide) is clearly the key variable in preparing high-area, X-ray indifferent aerogels [13,15], precursor concentration [13,14], the chemical nature of the non-aqueous solvent [14], and drying conditions [8,16,17] also play a role.

In this paper, we report our preparation of alumina and silica-doped alumina (9:1 Al:Si atom ratio) aerogels by supercritical drying of monolithic alcogels formed by slow, substoichiometric (H_2O:Al=2.2) hydrolysis of solutions of alkoxide precursors in an alcohol solvent. To understand the textural, structural and surface-chemical properties of the pure alumina aerogel, we first compare it with the well-known conventional aluminum oxidehydroxide and trihydroxide precursors and to a xerogel (the same monolithic alcogel dried by evaporation). This set of samples provides a firm basis for interpreting the effects of a well-dispersed silica dopant on the catalytically significant properties of the aerogel.

2. Methods

2.1. Sample preparation

To a beaker containing a mixture of 25 ml of *s*-butanol (Fisher, certified) and 9.4 ml of aluminum *s*-butoxide (ASB-Alfa), a second solution of 2.54 ml nitric acid (Baker, 70 w/w in water) in 10 ml *s*-butanol was added. The combined solution was clear. After mixing with a mechanical stir-bar for 25 min, 0.4 ml of distilled water was added over a 4 min period, 0.1 ml each minute, to reach a final overall hydrolysis ratio of 2.2 mol H_2O/mol ASB. (Overall ASB:H_2O:HNO_3:*s*-BuOH molar ratios were 1.0:2.2:1.1:10.) The solution gelled to a transparent, slightly yellow monolithic alcogel approximately 2 min after addition of the final water. The silica-doped alcogel was prepared in a similar manner, except that half way through the 25 min stirring period, 0.87 ml of tetraethyl orthosilicate (TEOS, Aldrich) was added to give an atomic ratio of 1:9 Si:Al. The mixed oxide alcogel gelled in about 5 min; its appearance was similar to that of the undoped alcogel.

For both alcogels, 'stepwise' addition of water and low pH were required to slow hydrolysis rates sufficiently to prevent the formation of precipitates. We also note that the mixed oxide recipe was designed specifically for promoting the homogeneous dispersion of the silica component. Slow co-hydrolysis of alkoxide mixtures has been demonstrated as an effective strategy for preparing the molecularly well-mixed aluminosilicates [18,19].

For preparation of aerogels, alcogels that had aged 2 h after gelling were dried by contact with supercritical carbon dioxide (343 K, $\sim 2.2 \times 10^4$ kPa) in a semi-continuous supercritical screening system (Autoclave Engineers model 08U-06-60FS). The alcohol solvent was completely removed over the course of about 2 h at a CO_2 flowrate of approximately 1400 sccm (ambient conditions). Product aerogels were ground to pass 100 mesh, then vacuum dried at 383 K (3 h) and then at 523 K (3 h) to remove physisorbed water and residual organics. Aerogel yield was low (roughly 2 g per preparation), so two batches of each were made. Generally we used one batch (denoted 'A') for structural and textural characterizations, and a second (denoted 'B') for surface-chemical characterizations. Cross checks of key measurements verified the repeatability of the preparations.

An alumina xerogel was prepared by drying a monolithic alcogel for 9 days in a nitrogen-purged glove box. During that time its volume decreased by approximately one-half. The gel was cut into smaller pieces (no dimension larger than ~1 cm) and dried in vacuum at 383 K for 3 h. The dried xerogel was ground to pass 100 mesh and subsequently dried at 523 K in vacuum for 3 h.

Samples of high purity bayerite and pseudoboehmite were provided by Alcoa. The as-received alumina precursors were vacuum dried at 383 K (3 h) and then at 523 K (3 h). Throughout the paper we refer to these materials as 'boehmite' and 'bayerite' and to materials derived from them by heat treatment as 'ex-boehmite' and 'ex-bayerite' despite the fact that we never observed a pure boehmite or bayerite phase.

Materials that had been dried at 523 K were calcined at 773 K for 2 h in flowing (~400 ccm) oxygen in a tube furnace. Similar calcinations at 973, 1173 and 1373 K were performed on samples that had been previously heated to 773 K. Heat treatment at 1473 K was performed (also on samples previously heated to 773 K) in a MoS_2 box furnace for 2 h in a static air environment.

2.2. Sample characterization

Crystalline structures were determined by powder X-ray diffraction (XRD) experiments performed on a Rigaku D/Max diffractometer (Cu K_α radiation). BET surface areas, pore volumes, and pore size distributions were measured by nitrogen adsorption/desorption using a Quantachrome Autosorb-1 system. Samples dried at 523 K were characterized by differential thermal analysis (10 K/min in ~50 ccm flowing He) using a Perkin-Elmer 1700 high-temperature thermal analyzr.

Solid-state nuclear magnetic resonance (NMR) studies were performed on a Bruker AM300 spectrometer modified with a high-power amplifier bay for solid capabilities. Samples (calcined at 773 K) were spun at the magic angle in 4 mm zirconia rotors at a typical speed of 8 kHz. ^{27}Al at 27 MHz power was set for a $\pi/8$ nutation, typically 4 μs. A recycle delay of 0.5 s was used between scans. The chemical shifts were externally referenced to a dilute solution of $Al(NO_3)_3$ at 0.0 ppm.

Samples calcined at 773 K were evaluated as catalysts for isomerization of 1-butene. Approximately 200 mg of sample was loaded to a downflow, fixed-bed reactor [20]. The sample was first dried at 473 K in 50 sccm He (Matheson HP) for 1 h. The bed temperature was lowered to 423 K and the feed switched to a mixture of 5 sccm 1-butene (Matheson, research grade) and 95 sccm helium. Isomerization products, *cis*- and *trans*-2-butene, were quantified by gas chromatography (Gow-Mac 550P with thermal conductivity detector; Supelco 23% SP1700 on 80/20 Chromosorb column). We report activity as areal reaction rate at 5 min on-stream time.

Aluminas calcined at 773 K were also characterized by Diffuse Reflectance Infrared Fourier Transform (DRIFT) spectroscopy using a Mattson Galaxy 5020 FTIR and a Harrick diffuse reflectance attachment. With a DTGS detector, spectra were collected between 400 and 4000 cm^{-1} with a resolution of 2 cm^{-1}. In an ex situ experiment (primarily for probing the skeletal vibration portion of the spectrum, between $\sim$400 and 1200 cm^{-1}), the sample was diluted with KBr ($\approx$2 wt.% sample) and the spectrum was collected at ambient conditions, with no special pretreatment. For in situ experiments, the sample was diluted with KBr ($\sim$5 wt.% sample) and placed inside a Harrick reaction chamber. The sample was heated to 473 K; the drying temperature used in the isomerization studies, in flowing helium and held there for 5 min, then its temperature was lowered to 383 K. Next, the helium flow was diverted through a pyridine saturator for 15 min. After pyridine dosing, the sample temperature was raised to 423 K, the reaction temperature employed during the isomerization studies, and a spectrum was collected to verify the presence and type (Lewis vs. Brønsted) of surface acid sites. Finally, the sample was heated to 673 K, a temperature at which all pyridine had desorbed, and a final spectrum was collected for evaluation of its hydroxyl inventory.

3. Results

3.1. Structural properties

X-ray diffraction patterns for Alcoa bayerite as a function of heat treatment temperature appear in Fig. 1. At the lowest temperature (523 K), the sample is already a mixture of bayerite, boehmite and a transition alumina (most likely η). The material is η at 773, γ at 1173, a mixture of θ and α at 1373, and finally, exclusively α at 1473 K. This sequence is typical of bayerite alumina precursors [1,2,4]. Alcoa boehmite displays a pseudoboehmite pattern at 523 K, as shown in Fig. 2. At 773 K, it exhibits a transition form pattern-η and possibly γ; it is clearly γ at 1173 K. The pseudoboehmite crystallizes to α at 1373 K. Its transformation sequence is similar to those reported for other pseudoboehmite samples [1,2,4].

As illustrated in Fig. 3, the aerogel's structural evolution differs significantly from those of the bayerite/boehmite pair. The supercritically dried and 383 K vacuum dried materials are essentially X-ray indifferent, exhibiting only very broad features below 2θ=30° (spikes near $\sim$42° and 49° are from the sample holder). While we cannot make a definite assignment, we believe they could arise from boehmite-like short-range order, similar to that reported for alumina precursors prepared in glycol environments [21,22]. From 523 K through 973 K, the X-ray patterns of the aerogel display no features. The aerogel exhibits a pattern characteristic of the η transition form at 1173 K. At 1373 K, α is just beginning to appear; at 1473 K the aerogel is exclusively α.

Introduction of silica (1:9 Si:Al) to form an alumina-silica co-gel does not affect the low and moderate temperature XRD patterns, as shown in Fig. 4. Note however, that the first appearance of α is delayed by about 100 K, from 1373 to 1473 K (compare with Fig. 3). This result is consistent with other published reports of silica doping in the same composition range [7,11,23,24]. The structural evolution of the alumina xerogel (Fig. 5) is similar to that of the pure alumina aerogel (Fig. 3). At 1373 K, the aerogel and the xerogel exhibit X-ray features characteristic of both α-alumina and a transition form, but the α reflections are significantly more intense in the xerogel sample. This difference suggests that crystallization of α has occurred to a greater extent, very likely having begun at a lower temperature, in the xerogel. Like the aerogel, initial ordering (as η) of the xerogel takes place upon calcination at 1173 K.

Materials that are *disordered* at 773 K (the aerogel, xerogel and silica-doped aerogel) display a single small exothermic DTA feature between 1050 and

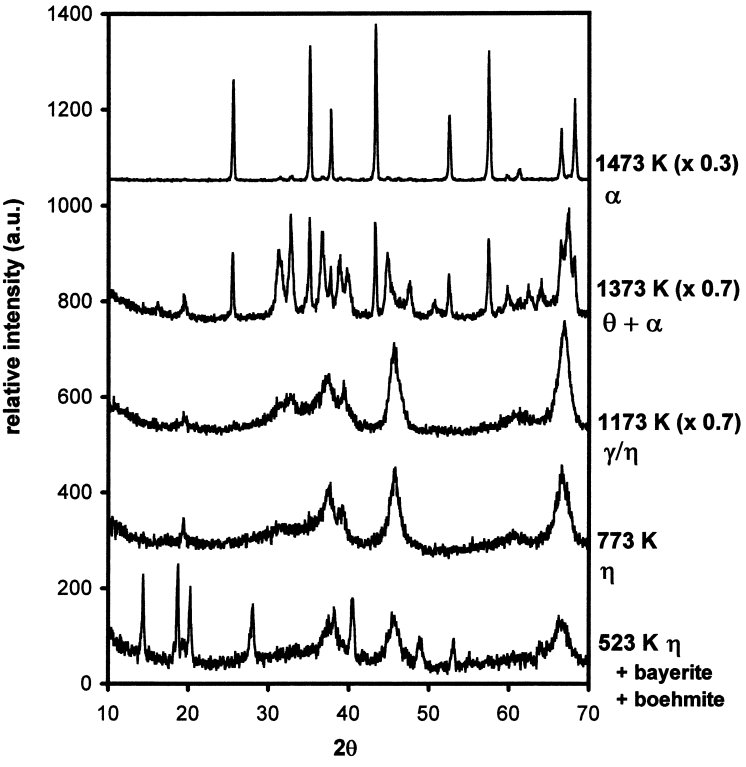

Fig. 1. X-ray diffraction (XRD) patterns (Cu K_α radiation) of Alcoa bayerite at different heat treatment temperatures. Sample was vacuum dried at 523 K, calcined in air at 1473 K and in oxygen for 2 h at other temperatures.

1150 K. In contrast, materials with transition alumina XRD patterns at 773 K (the ex-boehmite and ex-bayerite samples) do not exhibit this feature. The locations of the DTA exotherms are summarized in Table 1. In vacuum-dried precipitated alumina precursors, the exotherm has been linked to the amorphous-to-η transformation [25]. Consistent with this report, our X-ray indifferent materials order to η upon calcination at a temperature just slightly higher than those of the exotherms. (We note that the boehmite and bayerite samples *do not* exhibit a comparable exotherm upon conversion from the mono- or trihydroxide to transition alumina. These transformations are accompanied by the *endothermic* evolution of significant amounts of structural water.) For the silica-doped aerogel, the exotherm appears at ~11 K higher than in its undoped counterpart. The xerogel's exotherm appears at a temperature only marginally lower than in the aerogel.

Table 1
Differential thermal analysis (DTA) results

Sample	DTA exotherm[a] (K)
Aerogel [b]	1129
Silica-doped aerogel [b]	1140
Xerogel	1125
Ex-bayerite	None observed
Ex-boehmite	None observed

[a] DTA in flowing He (50 ccm) at 10 K/min on samples vacuum-dried at 523 K. Only features between 1050 and 1200 K are reported.
[b] Batch A.

Results of ^{27}Al MAS-NMR experiments performed on samples calcined at 773 K appear in Fig. 6. The ex-boehmite and ex-bayerite materials display features corresponding to tetrahedrally and octahedrally coordinated aluminum atoms (Al^{IV} at ~55 ppm and Al^{VI} at ~1 ppm), consistent with the spinel structure of the γ/η transition forms [1]. In addition to four and six coordination, the X-ray indifferent aerogels and

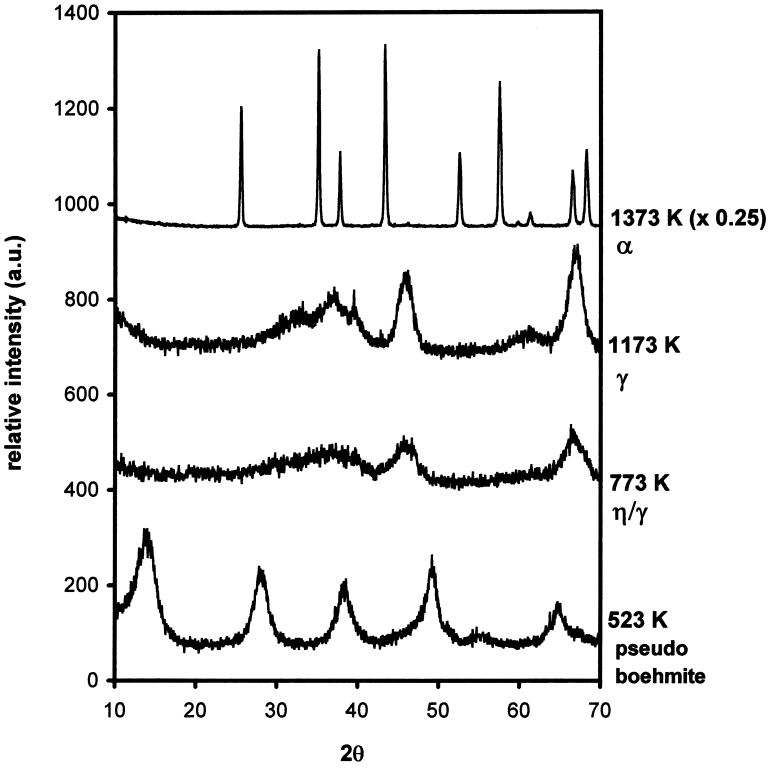

Fig. 2. X-ray diffraction (XRD) patterns (Cu K_α radiation) of Alcoa pseudoboehmite at different heat treatment temperatures. Sample was vacuum dried at 523 K, calcined in oxygen for 2 h at higher temperatures.

xerogel also possess penta-coordinated aluminum atoms (Al^V at ~27 ppm). Note that, upon heating to 1173 K, the temperature at which it orders to the η form-Al^V has been eliminated and the aerogel's spectrum displays only the Al^{IV} and Al^{VI} features of the transition form. These results strongly suggest that penta-coordinated aluminum atoms are characteristic of the X-ray amorphous form of alumina.

Skeletal ex situ infrared spectra for samples calcined at 773 K appear in Fig. 7. The alkoxide-derived materials (X-ray indifferent at 773 K) exhibit a single, very broad feature that is symmetric about 670 cm^{-1}. The ex-bayerite/ex-boehmite materials (transition form at 773 K), in contrast, display intensities biased toward the lower wavenumber region. Consistent with what we observe for the ex-bayerite and ex-boehmite samples, the spectrum of γ alumina has been reported to have two broad, poorly-defined bands at approximately 600 (tetrahedral Al) and 800 cm^{-1} (octahedral Al) [16,26]. In the amorphous materials, these two bands are apparently still present, but now they are of comparable intensity. In view of the NMR data (Fig. 6), we suspect that the frequency range of skeletal vibrations involving Al^V overlap primarily with those involving Al^{VI}, resulting in the characteristic 'symmetric' shape of the amorphous samples' skeletal region. We also note that the spectra of the undoped aerogel and its silica-doped counterpart are, in essence, the same. In particular, the silica-doped material exhibits no new features in the silica network vibration region of the spectrum (~950–1200 cm^{-1}).

3.2. Textural properties

Surface areas of the aluminas as functions of heat treatment temperature appear in Fig. 8. Below 1173 K, the undoped aerogel possesses the lowest surface areas of all the five samples. At 1373 and 1473 K, the aerogel possesses areas higher than the ex-boehmite, ex-bayerite and xerogel, illustrating the

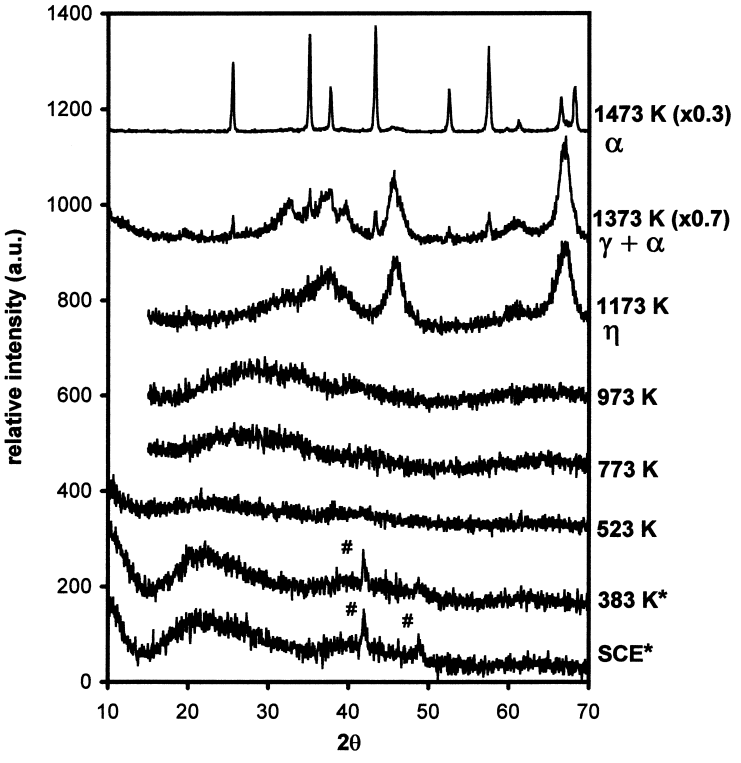

Fig. 3. X-ray diffraction (XRD) patterns (Cu K_α radiation) of alumina aerogel (batch A) at different heat treatment temperatures. Sample was vacuum dried at 383 and 523 K, calcined in air at 1473 K, and in oxygen for 2 h at other temperatures. * denotes material from a third batch of aerogel; # denotes reflections of brass sample holder.

ability of supercritical drying to preserve a strong, sintering-resistant network. Silica doping enhances aerogel area at all heat-treatment temperatures. Significantly, at 1473 K the silica doping increases the area of the aerogel from 30 to 60 m^2/g; this increase is directly related to silica's ability to delay crystallization to α. Finally, across the entire temperature range, we note that the xerogel follows the path of the bayerite and boehmite samples.

As illustrated in Fig. 9, the aerogels, which had the lowest areas upon moderate heat treatment, possess the highest pore volumes at all temperatures. Particularly notable are the high pore volumes of the silica-doped material. The low pore volume/high surface area of the xerogel, ex-boehmite and ex-bayerite materials are consistent with their pore-size distributions (Fig. 10); compared to the aerogels, this trio possesses very small pores. The aerogels are, in contrast, clearly mesoporous, the silica-doped version with a substantial additional pore volume contribution at higher pore radii. Note that, as was the case with surface area, the pore volume evolution and pore size distribution of the xerogel resemble those of the bayerite/boehmite-derived samples. The characteristic evolution pattern of the aerogels' textural properties appears, therefore, to be more a function of drying method than of the wet-chemistry used in their preparation.

3.3. Surface-chemical properties

Fig. 11 contains in-situ pyridine-region spectra (obtained at isomerization conditions) of samples calcined at 773 K. The amorphous materials adsorb very little pyridine, with the xerogel perhaps retaining slightly more than the aerogels. In each case, the pyridine signal is on a broad and variable background characteristic of the X-ray indifferent form; the domi-

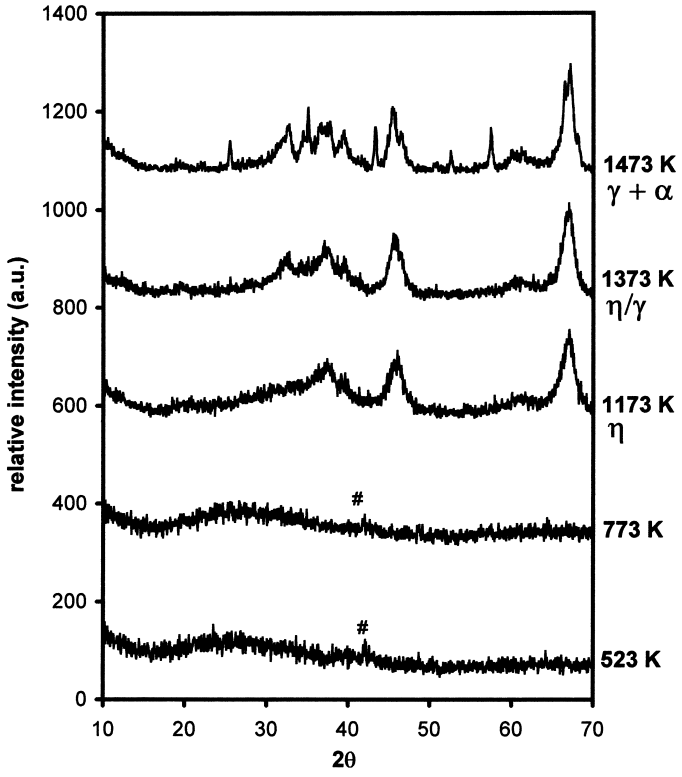

Fig. 4. X-ray diffraction (XRD) patterns (Cu K_α radiation) of silica-doped (9:1 Al:Si) alumina aerogel (batch A) at different heat treatment temperatures. Sample was vacuum dried at 523 K, calcined in air at 1473 K, and in oxygen for 2 h at other temperatures. # denotes reflections of brass sample holder.

nant feature is observed at around 1450 cm^{-1}, suggesting that the pyridine is hydrogen-bonded to surface hydroxyl groups, or perhaps adsorbed at Lewis acid sites. In contrast, both the ex-bayerite and ex-boehmite samples adsorb significantly more pyridine, but only at Lewis sites, not Brønsted. This result does not necessarily imply that there are no Brønsted sites on any of these materials. Alumina's Brønsted sites may be too weak to protonate pyridine, but perhaps capable of protonating a stronger base like ammonia [27].

Fig. 12 illustrates that at 673 K, both aerogels calcined at 773 K have very small hydroxyl populations. The silica-doped aerogel is essentially the same as the pure alumina aerogel in the hydroxyl region. Most notably, the mixed oxide exhibits no feature at $\sim$3750 cm^{-1} (the SiO–H stretch) that would suggest the presence of surface-segregated silica. Compared to the aerogels, the xerogel exhibits a significantly richer IR hydroxyl region with some spectrum definition. The broad peaks do not, however, appear at positions that have been previously assigned in the literature. Finally, we note that, even after heating to 673 K, the ex-bayerite and ex-boehmite materials retain relatively large hydroxyl contents.

Catalytic activities for isomerization of 1-butene for samples calcined at 773 K are given in Table 2. Neither aerogel is active for the isomerization of 1-butene; the remaining materials are only weakly active. We have, for example, previously reported the isomerization rates for mixed zirconia–silica aerogels that are approximately an order of magnitude higher than those in Table 2 [28]. The ex-bayerite material is active with a moderately high *cis/trans* product isomer ratio (3.0), which can be indicative of isomerization at a basic site via a carbanionic intermediate [29]. The ex-boehmite material is only very weakly active with an unquantifiable, but clearly greater than 1.0 product

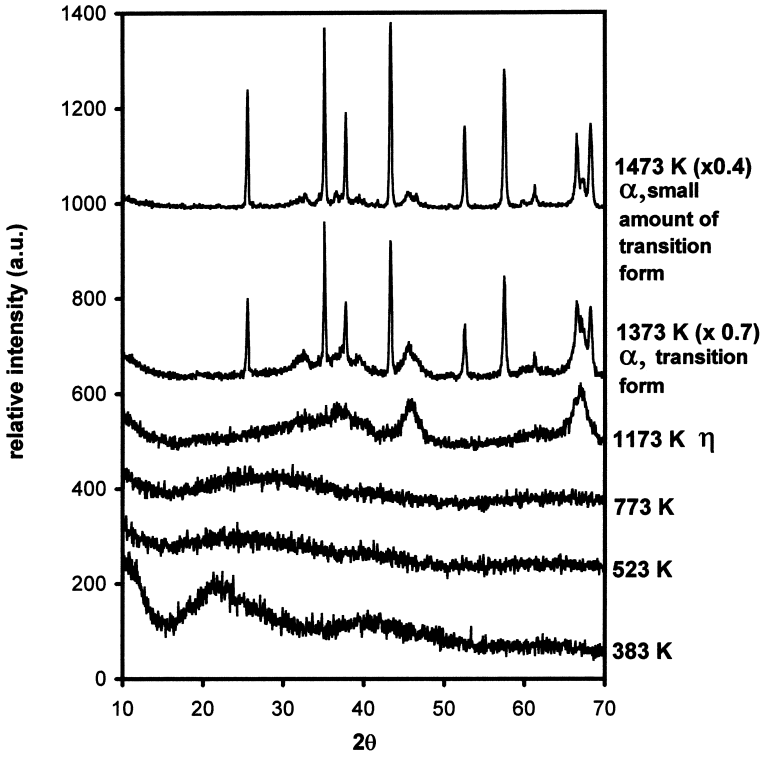

Fig. 5. X-ray diffraction (XRD) patterns (Cu K_α radiation) of alumina xerogel at different heat treatment temperatures. Sample was vacuum dried at 383 and 523 K, calcined in air at 1473 K, and in oxygen for 2 h at other temperatures.

Table 2
1-butene isomerization activity of aluminas calcined at 773 K

Sample ID	Isomerization rate (mmol/m^2/h) [a]	Product isomer ratio (*cis*/*trans*-2-butene) [a]
Aerogel (B)	0 [b]	–
Silica-doped aerogel (B)	0 [b]	–
Xerogel	0.011	1.4
Ex-bayerite	0.033	3.0
Ex-boehmite	0.002[c]	>1 [d]

[a] Recorded at 5 min time on stream; reaction conditions: 423 K, 1.0 atm, 95 sccm He, 5 sccm 1-butene, ~200 mg sample.
[b] No measurable activity.
[c] Estimated by difference (1-butene in reactor inlet minus 1-butene in reactor outlet).
[d]Not quantifiable; visual inspection suggests that *cis* integrator peak is larger than *trans*.

isomer ratio. Perhaps most interesting is that the xerogel, unlike the aerogels, does catalyze the isomerization reaction. Its product isomer ratio is only 1.4, not so far in excess of 1.0 to rule out the participation of Brønsted acid sites. We note that at comparable conversions, the xerogel and bayerite exhibit significantly different isomer ratios, suggesting that the active sites in these two cases are different.

4. Discussion

4.1. Structure of the alumina aerogel

Before either supercritical or evaporative drying, our alcogel is a transparent monolith. This observation provides two important clues about its microstructure. First, discrete 'primary particles', the first condensation products of the partially hydrolyzed precursor, are small, too small to scatter light. Second, the pre-oxide network possesses a high degree of connectivity; in other words, its structure is fairly mature prior to supercritical drying. This evidence is consistent with

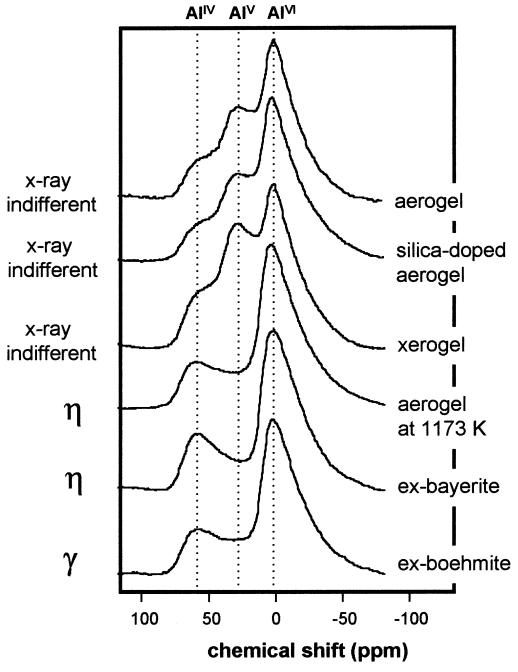

Fig. 6. ^{27}Al NMR spectra of alumina precursor samples calcined at 773 K (unless otherwise noted) in oxygen for 2 h. From top to bottom, the spectra are for aerogel (batch B), silica-doped aerogel (batch A), xerogel, aerogel at 1173 K, ex-bayerite, and ex-boehmite.

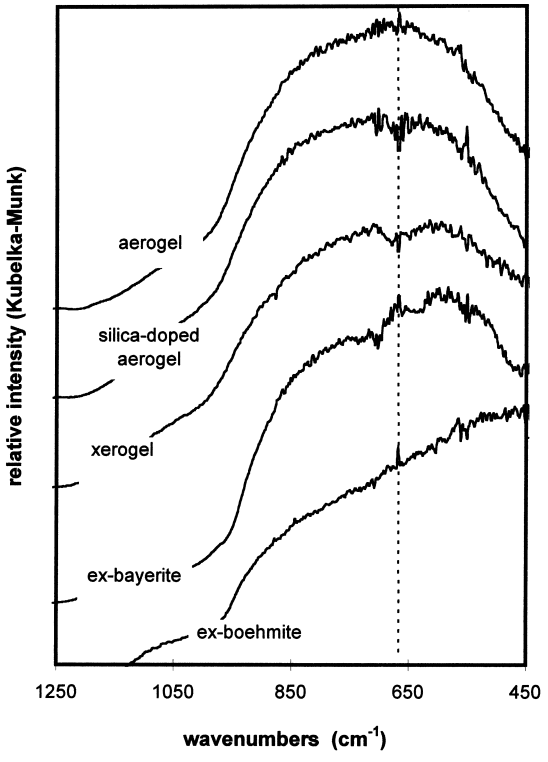

Fig. 7. Skeletal region ex situ DRIFT spectra of alumina precursor samples calcined at 773 K in oxygen for 2 h. From top to bottom, the spectra are for aerogel (batch A), silica-doped aerogel (batch A), xerogel, ex-bayerite, and ex-boehmite. Reference line at 670 cm^{-1}.

the formation of the pre-oxide network by a random polymerization process, one that we might expect to deliver an X-ray indifferent material. Controlled hydrolysis of alkoxides followed by supercritical drying is not limited to synthesis of alumina precursors; we have previously reported our application of this strategy for the preparation of a family of kinetically stabilized, X-ray amorphous single [30,31] and mixed [28,32] oxide aerogels.

The aerogel product is a pre-alumina that is X-ray indifferent over a very wide temperature range, at least through 973 K. The aerogel's structure transforms according to a specific, reproducible sequence: η at about 1173 K, α at about 1373 K. Other X-ray amorphous aluminas have been reported to transform according to similar sequences [13,14,25]; we therefore believe it to be characteristic of this form of alumina. Also characteristic of the X-ray amorphous alumina is the penta-coordinated aluminum, Al^V. We observed Al^V only in the X-ray indifferent samples; it was no longer present once the aerogel ordered as the η transition form (Fig. 6). It is very likely that the DTA exotherm that we (Table 1) and others [25] have observed to accompany the X-ray amorphous to η transformation arises from the energy released as the metastable Al^V of the amorphous form converts to the more stable Al^{VI} and Al^{IV} of the transition form. A similar link has been reported between Al^V conversion and the 1250 K DTA exotherm observed as molecularly well-mixed, X-ray amorphous aluminosilicate precursors crystallize to mullite [33–35].

The structural transformations of the X-ray indifferent aerogel differ significantly from those of the bayerite and boehmite precursors, both of which are ordered even at the lowest heat treatment temperatures. Of particular note is that the bayerite and boehmite precursors adopt transition form order at temperatures significantly lower than do the X-ray amorphous materials: ~800 vs. ~1200 K. This dif-

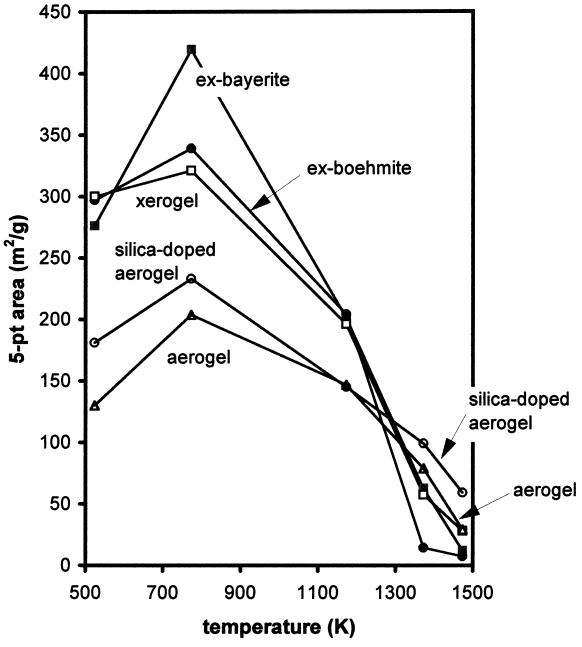

Fig. 8. Surface areas (5-point BET) of alumina precursors as functions of heat treatment temperature. Both aerogels are from batch A.

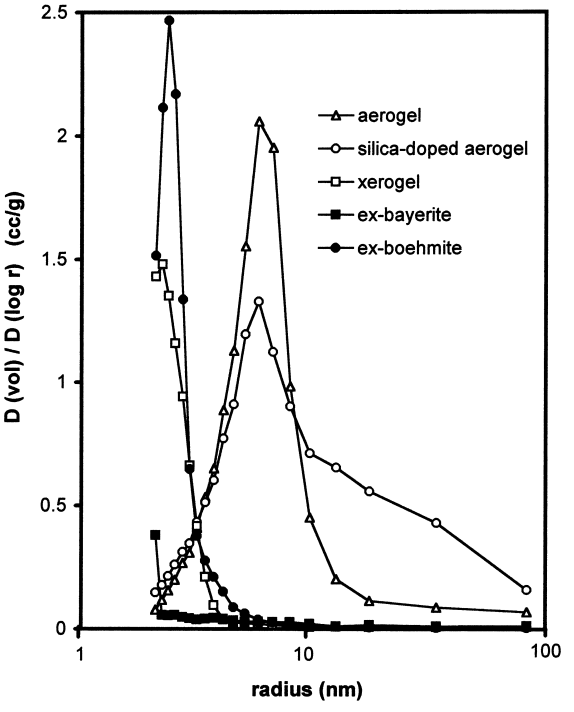

Fig. 10. Pore size distributions of alumina calcined at 773 K in oxygen for 2 h. Both aerogels are from batch A.

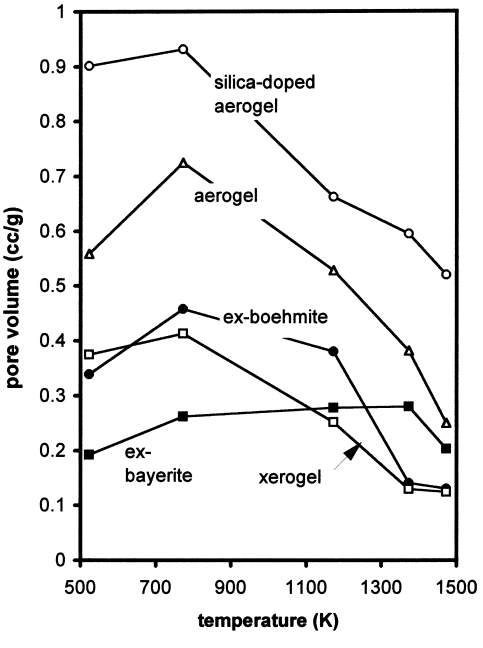

Fig. 9. Pore volumes of alumina precursors as functions of heat treatment temperature. Both aerogels are from batch A.

ference is due, in large part, to the topotactic nature of the transformation in the ordered precursors. The cubic close pack oxygen sub-lattice of the transition alumina already exists in the oxidehydroxide and trihydroxide precursors, requiring, therefore, only minor atomic rearrangement to attain the transition alumina structure. No similar order exists in the X-ray indifferent precursor, as evidenced by the presence of Al^V. Consequently, the amorphous precursor must undergo more extensive rearrangement, requiring higher temperatures, to order as a transition form. From this perspective, penta-coordinated aluminum can be viewed as a measure of oxygen lattice disorder, with Al^V atoms as defect sites.

4.2. *Comparison to other reported alumina aerogels*

Preparation of an X-ray amorphous aerogel depends upon the use of appropriate wet chemistry and drying conditions. To illustrate this point, in Table 3 we compare our aerogel to selected literature reports of

Table 3
Comparison of alumina aerogel preparations

Reference	BuOH (mols)	ASB (mols)	H_2O (mols)	Etacac (mols) [a]	HNO_3 (mols)	SCD[b] temp. (K)	Comments
This work	10	1	2.2	–	1.1	343	X-ray indifferent until 1173 K (η); converts to α at 1373 K; 204 m^2/g, 0.72 cc/g at 773 K.
Elaloui et al. [15]	13	1	3.0	2.0	0.5 [d]	308	X-ray indifferent until 1173 K (κ'); $\alpha+\kappa'$ at 1473 K; 369 m^2/g at 673 K
	0	1	67.0	–	0.2	533	Boehmite upon supercritical drying, δ or η at 1173 K, $\alpha+\theta$ at 1473 K, 178 m^2/g at 673 K
Teichner et al. [13]	30	1	3.0	–	–	543	X-ray indifferent until 1273 K ($\eta+\delta$) 239 m^2/g, 0.74 cc/g at 873 K
	30	1	$\geq$4.5	–	–	543	Some boehmite upon supercritical drying
	<20	1	3.0	–	–	543	Some boehmite upon supercritical drying
Mizushima and Hori [8,16,17,36]	12 [c]	1	3.0	1.0	–	543	Some pseudoboehmite/boehmite upon supercritical drying; γ until 1273 K, θ until 1473 K, then α; no Al^V
						353	Some γ upon supercritical drying; γ until 1373 K ($\theta+\alpha$); Al^V at both 673 and 873 K.
Ponthieu et al. [14]	160	1	3.0	–	–	543	X-ray indifferent until 673 K (η/γ); α at 1433 K; 370 m^2/g at 873 K.

[a] Ethyl acetoacetate.
[b] Supercritical drying temperature.
[c] Ethanol solvent.
[d] Acetic acid.

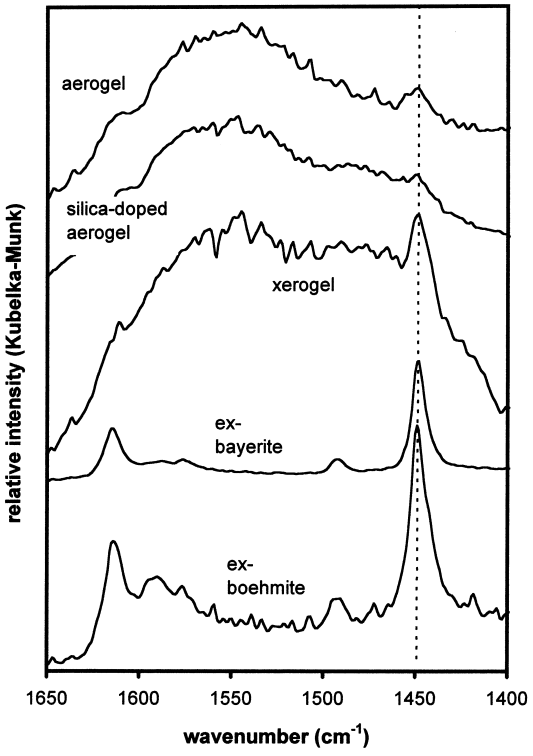

Fig. 11. In situ (423 K) DRIFT pyridine region spectra of alumina precursor samples calcined at 773 K in oxygen for 2 h. From top to bottom, the spectra are for aerogel (batch B), silica-doped aerogel (batch B), xerogel, ex-bayerite, and ex-boehmite. Each spectrum normalized to its skeletal region maximum.

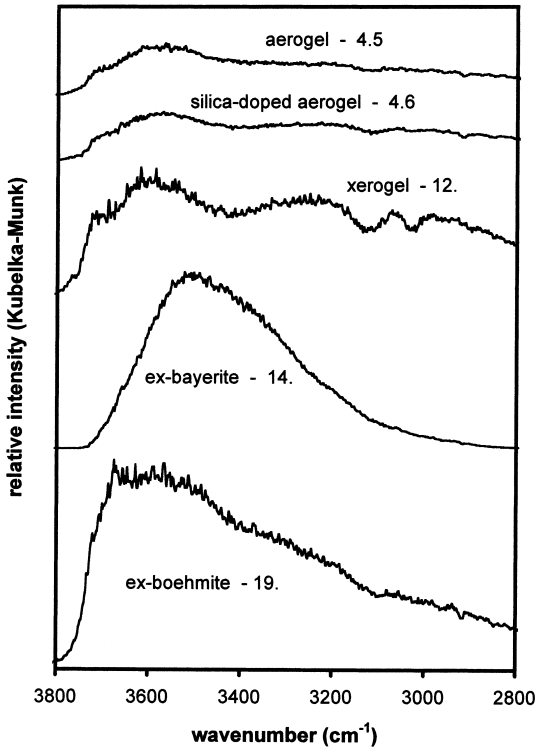

Fig. 12. In situ (673 K) DRIFT hydroxyl region spectra of alumina precursor samples calcined at 773 K in oxygen for 2 h. From top to bottom, the spectra are for aerogel (batch B), silica-doped aerogel (batch B), xerogel, ex-bayerite, and ex-boehmite. Numbers indicate relative integrated areas (linear background, each spectrum normalized to its skeletal region maximum) between 2800 and 3800 cm^{-1}.

alumina aerogels prepared from aluminum *s*-butoxide (ASB, the same precursor used in this work) in alcoholic solvents.

Elaloui et al. [15] have recently reported results for a pair of alumina aerogels that clearly demonstrate that not all preparations deliver an X-ray amorphous product. One, with concentrations, hydrolysis ratio, and drying temperature near to those we employed, resulted in an aerogel that, like ours, was X-ray indifferent until 1173 K. However, when the hydrolysis ratio was increased to well above stoichiometric and drying temperature increased from 308 to 533 K, the initial product of drying was a well-ordered boehmite.

The X-ray amorphous aerogel reported by Teichner et al. [13] is structurally and texturally very similar to our own material: it has comparable surface area and transforms according to a similar sequence. However, when either water ratio was increased to above stoichiometric (with respect to trihydroxide) or precursor concentration was significantly increased, their raw aerogel product displayed boehmite-like order, consistent with the results of Elaloui et al. [15]. Teichner et al. associated order with the presence of free water during the high-temperature drying step. In the high precursor concentration case, they explained the presence of excess water as the result of incomplete incorporation of reactant water into the structure of the pre-oxide; we believe this could be related to the increased hydrolysis rates that accompany higher precursor concentrations. Interestingly, Teichner et al.'s results suggest that our precursor concentration

could be high enough to encourage the formation of an ordered aerogel. However, our aerogel differs from their high precursor concentration case in two significant ways that allow our material to remain X-ray amorphous. First, we start with *sub*-stoichiometric water, thereby limiting the potential for excess water to remain, regardless of the reaction rates. Second, the slow hydrolysis process that we employ, moderated by addition of the nitric acid and stepwise water addition, may encourage the complete reaction of water.

Mizushima and Hori's aerogels [8,16,17] were prepared at high ASB concentrations, which, as described in the previous paragraph, favors the incomplete reaction of water. In addition, modification of the ASB precursor with ethyl acetoacetate probably made it more difficult to hydrolyze, thereby further increasing the amount of unreacted water that could be present in the supercritical drying step. As a result, neither of their as-dried aerogels, one dried at 543 K and a second dried by displacement with supercritical CO_2 at 353 K, were X-ray indifferent. The *type* of order did vary, however, with supercritical drying temperature. High temperature drying delivered a material with boehmite-like order, similar to Teichner et al.'s high precursor concentration material. At 353 K, the raw aerogel displayed a weak transition form (η/γ) X-ray pattern. Significantly, the low temperature aerogel possessed penta-coordinated Al (by NMR) upon heat treatment at both 673 and 873 K; the 543 K dried material did not [36]. However, the relative amount of Al^V appearing in the Mizushima and Hori material appears to be substantially less than what we see in our own aerogels, which is an indication that the former is actually a *mixture* of the amorphous and transition forms. The absence of Al^V (and, by inference, absence of any 'amorphous' alumina) in the material dried at 543 K illustrates how elevated drying temperatures can accelerate sintering and structural transformations.

The aerogel of Ponthieu et al. [14] is X-ray indifferent upon supercritical drying at 543 K, suggesting that free water was not present during the drying step. It does, however, transform to a transition alumina at a relatively low temperature. We suspect that low concentrations employed in this preparation may have suppressed hydrolysis rates enough to encourage more mature short-range order than in the other examples. While not detectable in XRD, the enhanced local order may have served to facilitate the X-ray amorphous to η transformation.

The key lesson of the comparison is that, while water ratio is an important variable, it alone cannot guarantee the preparation of an X-ray amorphous alumina. Pre-oxide network formation rates must be fast enough to 'trap' Al^V defects, but not so fast as to promote the incomplete incorporation of reactant water. Hence, we see the importance of not only water ratio, but also concentrations, pH and rate controlling additives like ethyl acetoacetate. Once formed, drying conditions dictate the fate of the X-ray amorphous network. Conditions that promote high water activity, high concentrations of 'free' water: high temperatures and high pressures, facilitate network ordering and conversion of Al^V.

4.3. *Supercritical drying's impact on structure and texture*

An important issue is the separation of those characteristics of the aerogel that are attributable to the wet-chemistry portion of its preparation from those that can be traced to the supercritical drying technique. Drying method has a large impact on the textural properties of the alumina precursor. Supercritical drying prevents pore collapse from high differential capillary pressures to deliver an aerogel that is clearly mesoporous (Fig. 10), with large pore volume (Fig. 9). The xerogel, in contrast, possesses much smaller pores, resulting in higher surface area, but low pore volume. Mizushima and Hori [8,17] and Elaloui et al. [15] reported similar differences between their alumina aerogels and xerogels. We note that the similarity between the the textural properties of the xerogel and the bayerite- and boehmite-derived materials is probably coincidental. Recall that the ex-boehmite and ex-bayerite owe their porosities to the elimination of structural water during topotactic transformations. The xerogel's small pores, on the other hand, result from macrostructural collapse during solvent removal.

Drying technique does not, however, affect atomic-level structure. Both the alumina aerogel (Fig. 3) and xerogel (Fig. 5) transform according to the same sequence; at 773 K, both are X-ray indifferent with substantial Al^V populations (Fig. 6). Apparently, water activity was not high enough with either drying

method to affect conversion of Al^V. Furthermore, as noted in the Section 3, crystallization of α appears to be slightly more facile in the xerogel. A higher density of primary particle contact points, which can act as seeds for α-crystallization [37], may exist in the denser (less porous) xerogel.

4.4. Surface-chemical/catalytic properties

Relative to the 'ordered' ex-boehmite and ex-bayerite materials, the X-ray amorphous aerogels (both silica doped and undoped) are characterized by the low Lewis acidity (sites accessible by pyridine at 423 K, see Fig. 11), and low surface hydroxyl content (at 673 K, see Fig. 12). Likewise, unlike the ordered materials, neither aerogel displays activity for 1-butene isomerization (Table 2). However, we are careful not to conclude that these properties are characteristic of amorphous alumina. The xerogel, which, like the aerogels, is X-ray indifferent at 773 K, adsorbs slightly more pyridine than the aerogels and displays a significantly richer IR hydroxyl region. More significantly, the xerogel is active in 1-butene isomerization, more active than the boehmite sample.

Butene isomerization probably does not probe a single surface property of alumina [38]. Aluminas are known to simultaneously possess acidic, basic, oxidizing and reducing sites [1,2,39]. Alkene isomerization activity has been attributed to acid–base pairs [40] and has been observed to correlate with both the oxidizing and reducing character of alumina [41]. Within this context, we make the following general observations. Because the xerogel is active with a *cis/trans* product isomer ratio only slightly greater than 1.0, we suspect that Brønsted sites (perhaps weak ones, since we are unable to probe them with pyridine at 423 K) participate in the reaction. At comparable conversions, the ex-bayerite sample is active with a significantly higher *cis/trans* ratio, suggesting participation of a different type of site(s), perhaps one with a significantly basic character. We cannot quantify the isomer ratio over the ex-boehmite material, but it appears to be comparable to that of ex-bayerite. Interestingly, we note that the property that best predicts isomerization activity in the sample set is the amount of strongly bound hydroxyl groups: materials with higher hydroxyl contents are the same ones that are active. It is possible that hydroxyl groups provide a weak Brønsted functionality that participates in the reaction mechanism.

Particularly interesting are the differences between the aerogel and the xerogel. While we cannot fully explain the ability of the xerogel to support a higher hydroxyl population than the aerogel (Fig. 12), we believe that it is related to a stronger interaction between –OH groups and the highly curved surfaces within the xerogel's smaller pores. The incrementally larger capacity of the xerogel to retain pyridine could, in turn, be due to the ability of the hydroxyl groups to hydrogen-bond with pyridine. Likewise, the enhanced hydroxyl content of the xerogel may also act as weak Brønsted acid sites that participate in the isomerization reaction.

We close this section with a discussion of the contribution of penta-coordinated aluminum on surface-chemical properties. Fripiat et al. have suggested that the metastability of linkages involving Al^V present electron-deficient sites, thereby enhancing the Lewis acid character of alumina surfaces [42]. Teichner and Van-Hoang, whose amorphous alumina precipitates presumably contain Al^V, noted a significant oxidizing/reducing character [41,43]. However, using pyridine adsorption, butene isomerization and hydroxyl inventory as probes, we find that our aerogels' surfaces are relatively inert. Furthermore, the aerogel/xerogel pair, both of which contain Al^V, exhibit significantly different chemical properties. In our aerogel samples, we suspect that either Al^V plays only a minor role in determining the surface chemistry, or perhaps that Al^V resides below the surface, allowing other factors to dominate.

4.5. Silica as a stabilizer of structure and texture

Perhaps the most important characteristic of our silica-doped alumina aerogel is the 'transparency' of its silica content. We saw no evidence of Si–O–Si network vibrations in its ex situ DRIFT spectrum (Fig. 7), consistent with the absence of large silica-rich domains in the sample. In contrast, 'segregated' 9:1 Al:Si aluminosilicates, such as examples prepared in our laboratory from commercially available colloidal sols ($\sim$10 nm diameter of silica 'primary particles') and by impregnation of a pure alumina aerogel with TEOS, exhibit strong silica network infrared

features [44,45]. We also note that the alumina skeletal region of the DRIFT spectrum is unperturbed by silica, implying that silicon atoms have not been incorporated into the alumina network to a significant extent. In other words, silicon is not a network former. Furthermore, silica does not suppress the formation of the penta-coordinated aluminum species that is characteristic of the X-ray amorphous form (Fig. 6). We infer, therefore, that silica has little impact on the processes that form the pre-alumina network during the slow co-hydrolysis step of the preparation. It is likely that silicon atoms are simply encapsulated randomly by the growing amorphous alumina, thereby assuring their homogeneous dispersion throughout the material.

The DTA results (Table 1) illustrate that the silica has a relatively modest impact on the initial ordering of the amorphous material to the η-alumina transition form, delaying it by 11 K. However, because they are homogeneously distributed throughout, but without actually participating in, the amorphous alumina matrix, silicon atoms are well-positioned to occupy vacancies in the spinel structure as the aerogel adopts transition form order. The potential for a high rate of vacancy occupation by silicon is very good, there is one vacancy per eight Al atoms in η-alumina [1], we dope with 1Si:9Al. Thus, the silicon dopant can effectively restrict Al atom diffusion through vacancies as a route for further sintering and phase transformations. Indeed, our results illustrate that silica doping (1:9 Si:Al) delays crystallization of the aerogel to α-alumina by 100 K (compare Figs. 3 and 4), thereby doubling surface area at 1473 K from 30 to 60 m^2/g.

Our observation that silica incorporated into the alumina aerogel by slow alkoxide co-hydrolysis has no impact on the surface chemical properties supports our conclusion that it is homogeneously dispersed throughout the sample. For example, while we find no evidence of a surface silanol (SiO–H) stretch in the silica-doped aerogel's hydroxyl region DRIFT spectrum (Fig. 12), aluminas doped by grafting silicon compounds onto their surfaces exhibit hydroxyl regions characteristic of silica [11,45]. And, unlike both the pure alumina aerogel and our homogeneously doped silica–alumina aerogel, we have observed that aluminas surface doped with molecular silicon precursors present significant populations of Brønsted acid sites and can be very active butene isomerization catalysts [45].

We note that silica dopants grafted onto the surface of aluminas by techniques such as incipient wetness impregnation can also effectively stabilize surface areas and lower temperature structural forms [9,11,45], suggesting that the surface diffusion sintering mechanisms operate in parallel with bulk diffusion through vacancies. In fact, an alumina doped with both bulk and surface silica has been reported to be especially effective for preserving surface area upon high temperature heat treatment [9]. However, as described above, unlike well-dispersed silica dopants, surface grafting can lead to unwelcome modifications to the alumina's surface chemistry [5].

5. Conclusions

X-ray amorphous alumina aerogels can be viewed as aluminum oxide-hydroxides having significant populations of lattice defects that manifest themselves as Al^V. Comparison of the literature reports of alumina aerogels suggests that control of hydrolysis rates is key to building a pre-oxide network containing Al^V and that solvent removal at conditions of low water activity is required to preserve the network. Our preparation of an alumina aerogel by slow (low-pH, staged water addition), sub-stoichiometric (2.2 H_2O:Al) hydrolysis of an alcoholic solution of an alkoxide precursor, followed by supercritical drying meets these criteria, delivering material that is X-ray indifferent over a wide temperature range.

We used the aerogel preparation as the basis for assessing the ability of a silica dopant to control alumina's textural and structural evolution. Slow co-hydrolysis of a mixture of Si and Al alkoxide precursors delivered an aluminosilicate aerogel (9:1 Al:Si) with very highly dispersed silica. In this technique, silicon atoms are randomly encapsulated by the growing pre-oxide network, available to occupy lattice vacancies as the alumina orders to the η transition form upon calcination at 1173 K. So positioned, silicon atoms can effectively restrict Al diffusion through vacancies as a mechanism for the further sintering of the transition alumina: crystallization of α-alumina is delayed from 1373 in the pure alumina aerogel to 1473 K in the silica-doped aerogel.

Significantly, silica's presence affects neither the amorphous alumina's hydroxyl inventory (at 673 K) nor its inertness towards 1-butene isomerization and pyridine chemical probes (at 423 K). The ability of a well-dispersed silica dopant to retard sintering without altering the surface-chemical properties contrasts with the reported behavior of aluminas modified by surface-grafted silica. The latter class of materials can exhibit enhanced surface acidities and surface hydroxyl inventories characteristic of silica, properties that are undesired in some applications.

Acknowledgements

We thank Professor Mark Davis and Dr. Larry Beck at the California Institute of Technology for performing the ^{27}Al NMR experiments. We also thank Mr. Mark Weaver and Dr. Neal Dando of the Alcoa Technical Center for providing the bayerite and pseudoboehmite samples. This work is supported by the Division of Chemical Sciences, Office of Basic Energy Sciences, Office of Energy Research and the U.S. Department of Energy (Grant No. DE-FG02-93ER14345).

References

[1] K. Wefers, C. Misra, Oxides and Hydroxides of Alumina, Alcoa Laboratories, 1987.
[2] B.C. Lippens, Physical and Chemical Aspects of Adsorbents and Catalysts, in: B.G. Linsen, J.M.H. Fortuin, C.O. Kerse, J.J. Steggerda (Eds.), Academic Press, New York, 1970, p. 177.
[3] R.B. Bagwell, G.L. Messing, Key Eng. Mater. 115 (1996) 45.
[4] W.H. Gitzen, Alumina as a Ceramic Material, American Chemical Society, Columbus, OH, 1970.
[5] C.K. Narlua, J.E. Allison, D.R. Bauer, H.S. Ghandi, Chem. Mater. 8 (1996) 984.
[6] M.F.M. Zwinkels, S.V. Jaras, P.G. Menon, Catal. Rev. -Sci. Eng. 35(3) (1993) 319.
[7] B.E. Yoldas, J. Mater. Sci. 11 (1976) 465.
[8] Y. Mizushima, M. Hori, J. Mater. Res. 8(11) (1993) 2993.
[9] L.L. Murrell, N.C. Dispenziere Jr., J. Catal. 111 (1988) 450.
[10] M.F.L. Johnson, J. Catal. 123 (1990) 245.
[11] B. Beguin, E. Garbowski, M. Primet, J. Catal. 127 (1991) 595.
[12] C.J. Brinker, G. Scherer, Sol–gel Science: The Chemistry and Physics of Sol–gel Processing, Academic Press, Boston, MA, 1990.
[13] S.J. Teichner, G.A. Nicolaon, M.A. Vicarini, G.E.E. Gardes, Adv. Colloid Interface Sci. 5 (1976) 245.
[14] E. Ponthieu, E. Payen, J. Grimblot, Sol–gel Processing and Applications, in: Y.A. Attia (Ed.), Plenum Press, New York, 1994 p. 221.
[15] A.E. Elaloui, A.C. Pierre, G.M. Pajonk, J. Catal. 166 (1997) 340.
[16] Y. Mizushima, M. Hori, J. Non-Cryst. Solids 167 (1994) 1.
[17] Y. Mizushima, M. Hori, Eurogel 91, in: S. Vilminot, R. Nass, H. Schmidt (Eds.), Elsevier, Amsterdam, The Netherlands, 1992, p. 195.
[18] J.C. Pouxviel, J.P. Boilot, Ultrastructure Processing of Advanced Ceramics, in: J.D. MacKenzie, D.R. Ulrich (Eds.), Wiley, New York, 1988, p. 197.
[19] J.B. Miller, E.I. Ko, Catal. Today 35 (1997) 269.
[20] J.B. Miller, Ph.D. Thesis, Carnegie Mellon University, Pittsburgh, PA, 1995.
[21] M. Inoue, H. Kominami, T. Inui, J. Chem. Soc. Dalton Trans., 3331, 1991.
[22] M. Inoue, Y. Konda, T. Inui, Inorg. Chem. 27(2) (1988) 215.
[23] B.E. Yoldas, D.P. Partlow, J. Mater. Sci. 23 (1986) 1895.
[24] M. Inoue, H. Otsu, H. Komonami, T. Nakamura, T. Inue, J. Mater. Sci. Lett. 13 (1994) 787.
[25] C. Hoang-Van, S.J. Teichner, Bull. Chem. Soc. France 5 (1969) 1498.
[26] T. Assih, A. Ayral, M. Abenoza, J. Phalippou, J. Mater. Sci. 23 (1988) 3326.
[27] A.A. Davydov, Infrared Spectroscopy of Adsorbed Species on the Surface of Transition Metal Oxides, Wiley, New York, 1990.
[28] J.B. Miller, E.I. Ko, J. Catal. 159 (1996) 58.
[29] J. Goldwasser, W.K. Hall, J. Catal. 71 (1981) 381.
[30] D.A. Ward, E.I. Ko, Chem. Mater. 5 (1993) 956.
[31] L.K. Campbell, B.K. Na, E.I. Ko, Chem. Mater. 4 (1992) 1329.
[32] J.B. Miller, S.T. Johnston, E.I. Ko, J. Catal. 150 (1994) 311.
[33] C. Gerardin, S. Sundaresan, J. Benziger, A. Navrotsky, Chem. Mater. 6 (1994) 160.
[34] A. Taylor, D. Holland, J. Non-Cryst. Solids 152 (1993) 1.
[35] B.E. Yoldas, J. Mater. Sci. 27 (1992) 6667.
[36] Y. Mizushima, M. Hori, M. Sasaki, J. Mater. Res. 8(9) (1993) 2109.
[37] I.M. Tijburg, H. DeBruin, P.A. Elberse, J.W. Geus, J. Mater. Sci. 26 (1991) 5945.
[38] J.W. Hightower, W.K. Hall, J. Phys. Chem. 71(4) (1967) 1014.
[39] H.R. Gerberich, W.K. Hall, J. Catal. 5 (1966) 99.
[40] J.B. Peri, J. Phys. Chem. 69 (1965) 211.
[41] A. Ghorbel, C. Hoang-Van, S.J. Teichner, J. Catal. 30 (1973) 298.
[42] F.R. Chen, J.G. Davis, J.J. Fripiat, J. Catal. 133 (1992) 263.
[43] C. Hoang-Van, S.J. Teichner, J. Catal. 16 (1970) 69.
[44] S.J. Monaco, E.I. Ko, unpublished results.
[45] J.B. Miller, E.I. Ko, unpublished results.